Journal of Chromatography, 457 (1988) 43–53
Elsevier Science Publishers B.V., Amsterdam — Printed in The Netherlands

CHROM. 20 950

NUMERICAL SIMULATION OF COLUMN PERFORMANCE IN ION-EXCLUSION CHROMATOGRAPHY

BRONISŁAW K. GŁÓD*, ANDRZEJ PIASECKI and JANUSZ STAFIEJ
Polish Academy of Sciences, Institute of Physical Chemistry, Kasprzaka 44/52, 01-224 Warsaw (Poland)
(First received July 4th, 1988; revised manuscript received September 1st, 1988)

SUMMARY

The separation mechanism of acidic compounds in ion-exclusion chromatography has been described using two approaches. The first one is based on the global thermodynamic and chromatographic relationships, the other on a computer simulation of the column performance. Strong acids leave the column unseparated, within its dead volume, and weak acids appear at the end of the chromatogram also unseparated. It was found that the addition of an acidic compound eliminates the dependence of the retention volume on the sample concentration. By use of the computer simulations, the evolution of the chromatographic peaks with time and the peak shape for the sample analyzed have been studied. The results compare favourably with the experimental data available in the literature.

INTRODUCTION

Ion-exclusion chromatography (IEC) has been described as an efficient method for the separation of ionic species[1–8]. Qualitatively, the primary mechanism of separation is based on the following phenomenon: neutral molecules penetrate the cation exchange resin while anions are repulsed — in other words excluded from it[1]. This has been confirmed by Tanaka *et al.*[9] who have shown that the dependence of the distribution coefficient, K_d, on the pK_a values of various acidic compounds is analogous to the dependence of K_d on the logarithm of the molecular weight in size exclusion chromatography.

A more quantitative description of these findings has been attempted[10] and the following formula was derived:

$$K_d = [1 + 2c/K_a - (1 + 8c/K_a)^{1/2}]/(2c/K_a - 2) \quad (1)$$

where K_a is the dissociation constant of the acid analyzed and c is the maximum peak concentration of the sample. The latter quantity can be evaluated only approximately or has to be determined experimentally.

In this work we have developed a more accurate approach towards the quantitative description of the separation mechanism in IEC. In this approach some simplifying assumptions used when deriving eqn. 1 are abandoned; K_d cannot be

0021-9673/88/$03.50

expressed in a closed form as in eqn. 1 and has to be evaluated numerically as a function of the parameters characterizing the sample, the column, the mobile and the stationary phases. The influence of these parameters on K_d is the subject of the present study. The use of an acidic compound to buffer the mobile phase is advantageous in IEC in some instances because it eliminates the dependence of the distribution coefficient on the sample concentration. A numerical simulation of the column performance using the finite element method has also been performed. This method provides additional information on the influence of the above parameters on the peak shape.

For convenience all symbols used in this work are listed below:

c Overall concentration of the sample in the peak volume
c_i Sample concentration injected
c_b Buffer concentration
c_{bM} Buffer concentration in the mobile phase
c_{bS} Buffer concentration in the stationary phase
c_f Functional group concentration in the support
c_M Sample concentration in the mobile phase
c_S Sample concentration in the stationary phase
K_a Dissociation constant of compound analyzed
K_b Dissociation constant of buffering compound
K_d Global distribution coefficient
k_d Local distribution coefficient
K_f Dissociation constant of resin functional group
m Sample mass corresponding to a theoretical plate
m_b Buffer mass corresponding to a theoretical plate
N Number of theoretical plates of the column
V_i Sample volume injected
V_M Column dead volume
v_M V_M/N
V_P Peak volume
V_R Retention volume
V_S Inner volume of the column
v_S V_S/N

FORMULATION OF THE MODEL

The following assumptions are involved in our model.

(1) Homogeneity of the column, implying that the ratio of the volume of the mobile phase to the volume of the stationary phase, as well as the mobile phase flow-rate, are constant along the column length.

(2) The influence of the axial diffusion of the sample and kinetic effects can be neglected.

(3) The separation in IEC is dominated by a Donnan membrane equilibrium mechanism and can be described by the following set of equations [*cf.*, eqns. 3–7 of ref. 10]

$$[H^+]_M[R^-]_M[HR]_M = [H^+]_S[R^-]_S[HR]_S \quad (2)$$

$$[H^+]_M[B^-]_M[HB]_M = [H^+]_S[B^-]_S[HB]_S \quad (3)$$

$$K_a = [H^+]_M[R^-]_M/[HR]_M \quad (4)$$

$$K_b = [H^+]_M[B^-]_M/[HB]_M \quad (5)$$

$$K_f = [H^+]_S[F^-]_S/[HF]_S \quad (6)$$

$$[H^+]_M = [R^-]_M + [B^-]_M \quad (7)$$

$$[H^+]_S = [F^-]_S + [R^-]_S + [B^-]_S \quad (8)$$

$$[HR]_M = [HR]_S \quad (9)$$

$$[HB]_M = [HB]_S \quad (10)$$

where HR, HB and HF are the formulae of the sample acidic compound, of the acid used as a buffer and of the acidic functional group of the resin respectively. The subscripts M and S refer to the mobile phase and to the stationary phase respectively. In the above equations it is assumed that the properties of the solvent in the stationary phase are the same as those in the mobile phase.

The overall buffer and functional group concentrations can be expressed as

$$c_b = [B^-]_M + [HB]_M \quad (11)$$

$$c_f = [F^-]_S + [HF]_S \quad (12)$$

For a specified amount of the acidic sample, its equilibrium concentration in specified volumes of the mobile and the stationary phases can be calculated on the basis of eqns. 2–12 together with an additional equation expressing the mass conservation for the amount of sample.

In what we call the global approach, it is assumed that the equilibrium conditions apply to the peak volume of the sample:

$$V_P = V_R(2\pi/N)^{1/2} \quad (13)$$

Therefore the sample is distributed between the volumes of the two phases corresponding to the sample peak volume, as expressed by:

$$c_i V_i = \{V_S([R^-]_S + [HR]_S) + V_M([R^-]_M + [HR]_M)\}V_P/(V_M + V_S) \quad (14)$$

The analogous equation in ref. 10 is based on the implicit assumption that the volumes of the mobile and the stationary phases are equal. Eqn. 14 is the mass conservation equation, but the retention volume is not yet specified. In the global approach this can be done by considering the definition of the distribution coefficient and its relationship with the retention volume:

$$K_d = ([R^-]_S + [HR]_S)/([R^-]_M + [HR]_M) \quad (15)$$

$$K_d = (V_R - V_M)/V_S \quad (16)$$

The set of eqns. 2–16 can be solved with respect to the distribution coefficient, K_d, retention volume, V_R, peak volume, V_P, and the twelve concentrations: $[H^+]_M$, $[H^+]_S$, $[R^-]_M$, $[R^-]_S$, $[B^-]_S$, $[B^-]_M$, $[F^-]_S$, $[HR]_M$, $[HR]_S$, $[HB]_M$, $[HB]_S$, $[HF]_S$. The solution is in the form of functions of the parameters K_a, K_b, K_f,c_i, c_b, c_f, V_i, V_M, V_S and N. These functions cannot be obtained in a closed form and a numerical procedure is required. It is fairly simple for pure water as a mobile phase, and assuming complete dissociation of the functional groups in the stationary phase: $c_b = [HF]_S = 0$. If $c = c_i V_i/V_P$ denotes the overall concentration of the sample in the peak volume, then eqn. 14 can be rewritten as:

$$c = \{V_S([R^-]_S + [HR]_S) + V_M([R^-]_M + [HR]_M)\}/(V_M + V_S) \quad (17)$$

After some elementary algebra, eqns. 2–6, 11, 12 and 15–17) yield:

$$c = c_i V_i (N/2\pi)^{1/2}/(K_d V_S + V_M) \quad (18)$$

$$[R^-]_S = (cV_M - [R^-]_M V_M - [R^-]_M^2 V_M/K_a + cV_S - [R^-]_M^2 V_S/K_a)/V_S \quad (19)$$

$$[R^-]_M = {}^1/_2 K_a[1 + (4c/K_a)(V_M/V_{S+1})/(K_d + V_M/V_S)]^{1/2} - 1 \quad (20)$$

$$K_d = (V_M/V_S)(c - [R^-]_M - [R^-]_M^2/K_a) + c/([R^-]_M + [R^-]_M^2/K_a) \quad (21)$$

The above equations provide the necessary relations to determine the four unknown quantities: the distribution coefficient, peak concentration, c, and the concentrations $[R^-]_S$ and $[R^-]_M$, as functions of the other parameters. The numerical method adopted is as follows. An arbitrary value, say 1/2, is ascribed to K_d. On the basis of this value, c and the other unknowns are calculated (eqns. 18–20) as well as the next value of K_d (eqn. 21). The procedure is then repeated until self consistency is reached. The case of the buffered mobile phase can be treated in a similar fashion.

The global approach is inconsistent in that eqns. 2–10 generally determine a non-linear distribution isotherm, while the use of eqns. 13, 15 and 16 is justified only in the linear case. To eliminate this inconsistency a numerical simulation method has been devised in which eqns. 2–10 are applied locally to small fragments of the column corresponding roughly to theoretical plates. The portion of the mobile phase at such a plate is "equilibrated" with the portion of the stationary phase and then "moved" to the next plate simulating the passage of the sample. The "equilibration" amounts to a calculation of the distribution of the amount of the sample compound brought by the incoming portion of the mobile phase plus what remained in the stationary phase. This involves a recurrent procedure implying that the set of eqns. 2–10 and

$$c_S(i,j) = [R^-]_S + [HR]_S \quad (22)$$

$$c_M(i,j) = [R^-]_M + [HR]_M \quad (23)$$

$$m(i,j) = c_S(i-1,j)v_S + c_M(i-1,j-1)v_M \quad (24)$$

$$k_d(i,j) = c_S(i,j)/c_M(i,j) \quad (25)$$

$$c_{bM}(i,j) = [B^-]_M + [HB]_M \quad (26)$$

$$c_{bS}(i,j) = [B^-]_S + [HB]_S \quad (27)$$

$$m_b(i,j) = c_{bM}(i-1,j)v_M + c_{bS}(i-1,j-1)v_S \quad (28)$$

are solved at ith time step and jth plate with the following initial and boundary conditions

$$c_S(0,j) = c_M(0,j) = 0 \text{ for } j = 1, \ldots, N \quad (29)$$

$$c_{bM}(0,j) = c_b \text{ for } j = 1, \ldots, N \quad (30)$$

$$c_{bS}(0,j) = c_{bS}^0 \quad (31)$$

where c_{bS}^0 is the buffer concentration in the stationary phase at equilibrium with the mobile phase buffer at a concentration c_b. It can be calculated on the basis of eqns. 2–10 assuming the absence of the sample in the mobile phase:

$$c_M(i,0) = c_i \text{ for } i = 1, \ldots, V_i/v_m \quad (32)$$

$$c_M(i,0) = 0 \text{ for } i > V_i/v_m \quad (33)$$

$$c_{bM}(i,0) = c_b \text{ for all time steps} \quad (34)$$

The method is suitable for studying the peak evolution with time and its final shape.

RESULTS

Global approach, unbuffered mobile phase

At first we considered the influence of such parameters as c_i, K_a and c_f on the distribution coefficient. We assumed the following values[10]: $V_M = 800\ \mu l$, $V_S = 2000\ \mu l$, $V_i = 5\ \mu l$, $N = 1000$ and the complete functional group dissociation.

The dependence of the distribution coefficient on the sample concentration for several values of the acid dissociation constant and for the concentration of the functional groups, $c_f = 10^{-3}\ M$, is presented in Fig. 1. The distribution coefficient is a growing, S-shaped function of the sample concentration. For low and high sample concentrations, K_d is practically constant with the sample concentration. The K_d *vs.* c_i curves for values of K_a much less than c_f form a set of parallel curves, as is presented in Fig. 2 for several values of K_a and $c_f = 10^3\ M$. Also K_d is hardly dependent on c_f for K_a

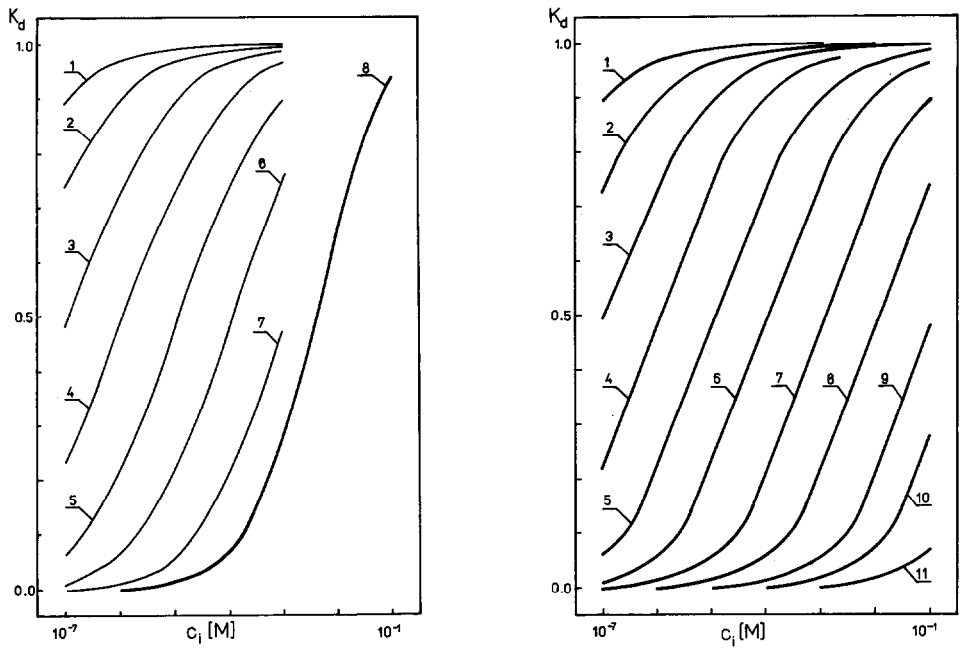

Fig. 1. Dependence of the distribution coefficient, K_d, on sample concentration, c_i, for a concentration of functional groups, $c_f = 10^{-3}$ M, and for several values of the acid dissociation constant, K_a: 1, 10^{-10}; 2, 10^{-9}; 3, 10^{-8}; 4, 10^{-7}; 5, 10^{-6}; 6, 10^{-5}; 7, 10^{-4}; 8, $\geqslant 10^{-3}$ M. $V_M = 800$ μl, $V_S = 2000$ μl, $V_i = 5$ μl, $N = 1000$.

Fig. 2. Dependence of K_d, on c_i for $c_f = 10^3$ M, and for several values of the acid dissociation constant, K_a: 1, 10^{-10}; 2, 10^{-9}; 3, 10^{-8}; 4, 10^{-7}; 5, 10^{-6}; 6, 10^{-5}; 7, 10^{-4}; 8, 10^{-3}; 9, 10^{-2}; 10, 10^{-1}; 11, 10^{0} M. Other conditions as in Fig. 1.

much less than c_f. When K_a is greater than c_f then the distribution coefficient is practically independent of the value of K_a up to the limit of a completely dissociated acid corresponding to the rightmost curve in Fig. 1. A set of these curves, *i.e.*, K_d *vs.* c_i curves for a completely dissociated acid, corresponding to different concentrations of the functional groups is presented in Fig. 3. The lower the c_f value the more pronounced and growing function is such a curve. However, K_a greater than c_f is rather a theoretical case since under normal chromatographic conditions c_i and K_a are much less than c_f.

The dependence of the distribution coefficient on the logarithm of the dissociation constant for various concentrations of the injected sample and the functional group concentration, $c_f = 10^{-3}$ M is presented in Fig. 4. If K_a is much less than c_f then K_d is a decreasing function of K_a (the leftmost part of Fig. 4). For higher values of the dissociation constant the distribution coefficient becomes a constant independent of K_a but dependent on c_i. It is worth noting that an increase in the sample concentration and a decrease in the dissociation constant have a similar effect — an increase of the K_d value. It is consistent with the fact that neutral molecules can penetrate the resin and in this way contribute to the increase in K_d.

The influence of the functional group concentration on the distribution coefficient has also been considered. For K_a and c_i much greater than c_f the distribution

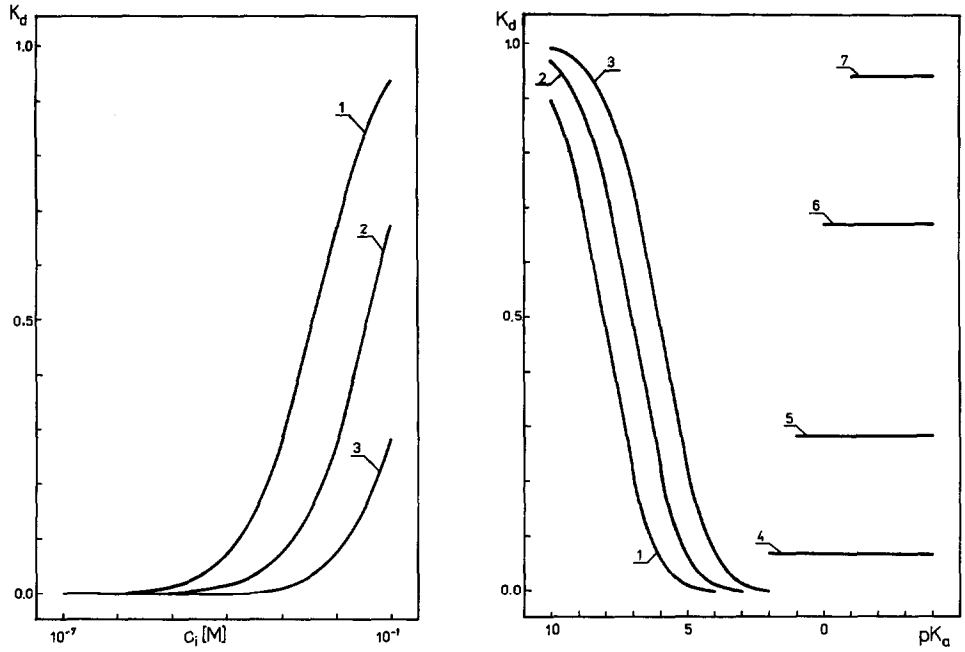

Fig. 3. Dependence of K_d on c_i for an acid dissociation constant, $K_a = 10^{-3}$ M and for several values of c_f: 1, 10^{-3}; 2, 10^{-2}; 3, 10^{-1} M. Other conditions as in Fig. 1.

Fig. 4. Dependence of K_d on the logarithm of the acid dissociation constant, pK_a for $c_f = 10^{-3}$ M, and for several values of the sample concentration, c_i: 1, 10^{-7}; 2, 10^{-6}; 3, 10^{-5}; 4, 10^{-4}; 5, 10^{-3}; 6, 10^{-2}; 7, 10^{-1} M. Other conditions as in Fig. 1.

coefficient is a decreasing function of c_f and K_d does not depend on K_a. However, for a normal chromatographic condition, K_a and c_i are much less than c_f, the distribution coefficient is independent of c_f and depends only on the ratio c_i/K_a. Therefore it is convenient to use reduced variables, c_i/K_a and c_f/K_a, instead of c_i, K_a and c_f, because the distribution coefficient depends only on two independent variables. The dependence of

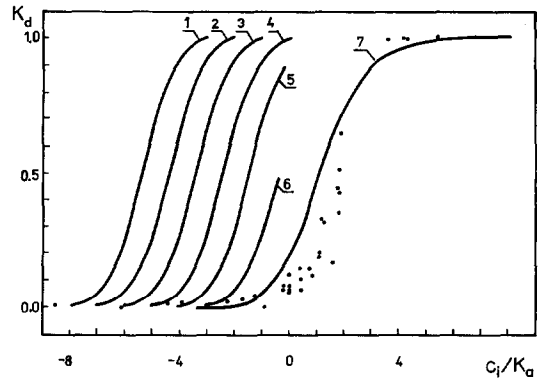

Fig. 5. Dependence of K_d on the quotient c_i/K_a for various values of c_f/K_a: 1, 10^{-6}; 2, 10^{-5}; 3, 10^{-4}; 4, 10^{-3}; 5, 10^{-2}; 6, 10^{-1}; 7, $\geqslant 10^{0}$. Points represent experimental values. Other conditions as in Fig. 1.

the distribution coefficient on c_i/K_a for various c_f/K_a is presented in Fig. 5. It is seen that K_d is a growing function of the quotient c_i/K_a. If we consider the usual chromatographic conditions when c_i is much greater than K_a then the decreasing function reduces to a constant one and the distribution coefficient depends only on c_i/K_a. This result is worth emphasizing since little effort is required to calculate the retention volume of any acid provided the parameters describing the column are known. The points in Fig. 5 correspond to the experimental data[10]. A good agreement with the theoretical calculations is observed. Analogous results were obtained for data presented in ref. 9.

The dependences of the distribution coefficient on the ratio c_f/K_a for several values of c_i/K_a are presented in Fig. 6. The distribution coefficient is a decreasing function of the ratio and it is practically zero when c_i is of the order of c_f or greater.

We have also considered the influence of the other experimental parameters on the distribution coefficient. An increase in the number of the theoretical plates, N, while keeping constant both V_S and V_M (and assuming that $c_f \gg c_i$ and $c_f \gg K_a$) results in a parallel shift of the K_d *vs.* c_i/K_a curve towards the stronger and more dilute acids. An increase in the ratio V_M/V_S while keeping constant N and $V_M + V_S$ results in a change of the slope of the curves K_d *vs.* c_i/K_a. In other words a change of the pK_a range of the separable acids is observed. An uniform increase in N, V_M and V_S (increase of the column length), *i.e.*, keeping $N/(V_M + V_S)$ and V_M/V_S constant, results in better separations over wider ranges of pK_a values of the acids analyzed.

Global approach, buffered mobile phase

The dependence of the distribution coefficient and the retention volume of the analyzed sample on the sample concentration injected is inconvenient from the analytical point of view. We have tried to eliminate it by the addition of a strongly acidic buffer to the mobile phase. Most important, from the practical point of view, is the dependence of the distribution coefficient on c_i and K_a. The dependence of the distribution coefficient on the sample concentration injected is presented in Fig. 7. The curves K_d *vs.* c_i or K_d *vs.* K_a are shifted towards more dilute and/or stronger acids when the buffering acidic compound is added to the mobile phase. It follows that the pK_a range of separable acids is also shifted in the same way. Therefore a change in the

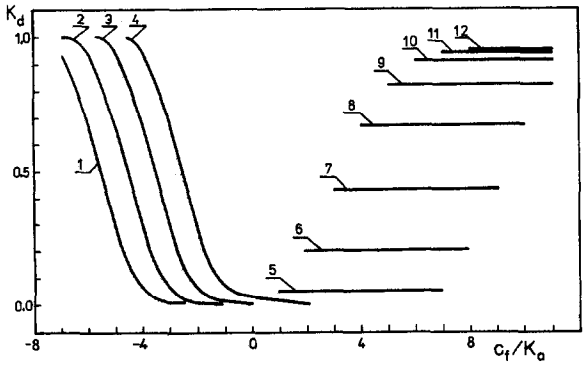

Fig. 6. Dependence of K_d on c_f/K_a for various values of c_i/K_a: 1, 10^{-5}; 2, 10^{-4}; 3, 10^{-3}; 4, 10^{-2}; 5, 10^{-1}; 6, 10^{0}; 7, 10^{1}; 8, 10^{2}; 9, 10^{3}; 10, 10^{4}; 11, 10^{5}; 12, 10^{6}. Other conditions as in Fig. 1.

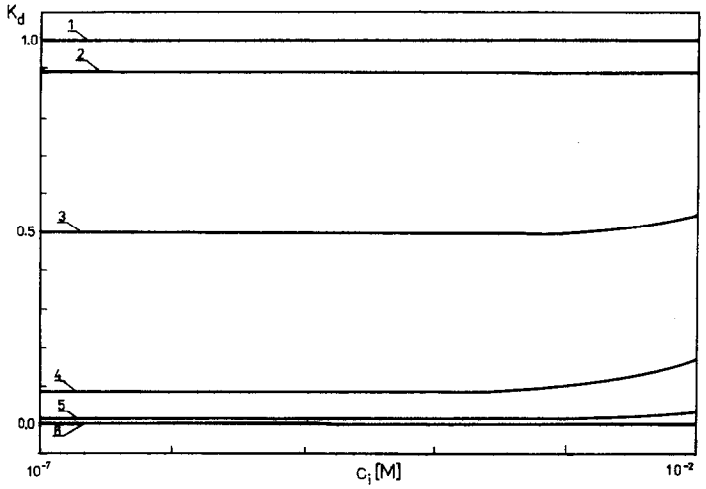

Fig. 7. Dependence of K_d on c_i for several values of K_a: 1, 10^{-5}; 2, 10^{-4}; 3, 10^{-3}; 4, 10^{-2}; 5, 10^{-1}; 6 = 10^{0}. $c_b = 10^{-3}$ M, $K_b = 10^3$, $c_f = 1$ M, $V_M = 800$ μl, $N = 1000$, $V_S = 2000$ μl, $V_i = 5$ μl.

buffer concentration or its dissociation constant can be used to control the retention volume, and consequently the separation, of the sample analyzed. Acids unseparated in pure water used as a mobile phase can be separated when a buffer is added. As is also seen in Fig. 7, the distribution coefficient is hardly dependent on the concentration of the sample injected when this concentration is lower than or approximately equal to the buffer concentration. This is advantageous from the analytical point of view.

The dependence of the distribution coefficient on the buffer concentration is a growing function as is seen in Fig. 8, for various values of K_a and for $c_i = 10^{-3}$ M. It can also be deduced from the figure that c_B, as well as K_b, can be used to control the range of pK_a of the acids analyzed. This behaviour is a result of the drawback of the dissociation of the analyzed sample caused by the addition of the buffer. The dependences of K_d on the other parameters are analogous to those for the unbuffered mobile phase.

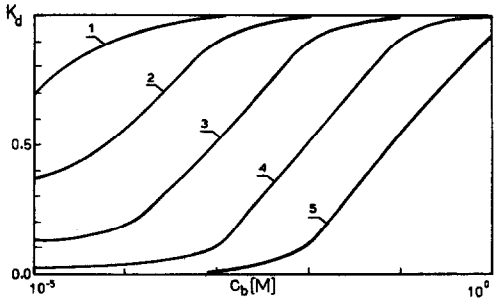

Fig. 8. Dependence of K_d on the buffer concentration, c_b, for several values of K_a: 1, 10^{-5}; 2, 10^{-4}; 3, 10^{-3}; 4, 10^{-2}; 5, 10^{-1} M. $c_i = 10^{-3}$ M. Other conditions as in Fig. 7.

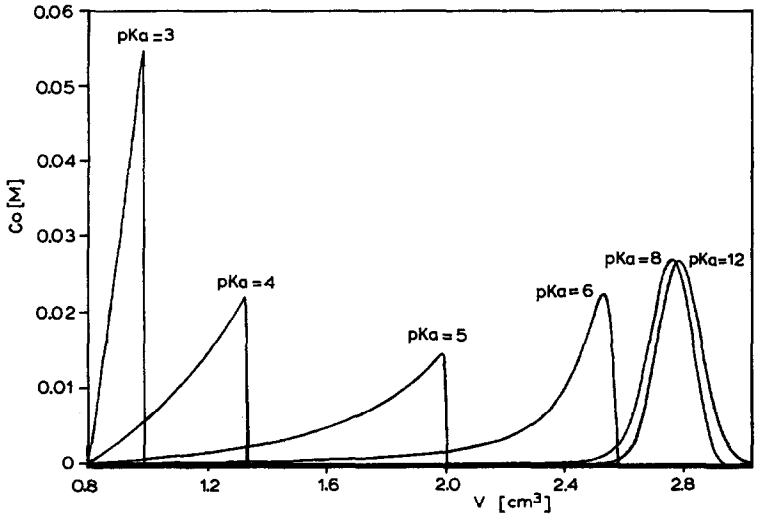

Fig. 9. Chromatograms of several acidic compounds (unbuffered mobile phase). $c_i = 10^{-3}$ M. Other conditions as in Fig. 1. $c_0 = c_M(i,N+1)$ —output concentration; $V = i \cdot v_M$ —elution volume.

Computer column modelling

The results of the computer simulation are presented in the form of calculated concentration profiles in Figs. 9 and 10 for unbuffered and buffered mobile phases respectively and for several values of pK_a of the acids analyzed. In the case of an unbuffered mobile phase the concentration profiles assume the form of leading peaks, except for the strongest and the weakest acids which form fairly symmetrical peaks. As was mentioned in the previous paragraph, after addition of a buffer the stronger acids

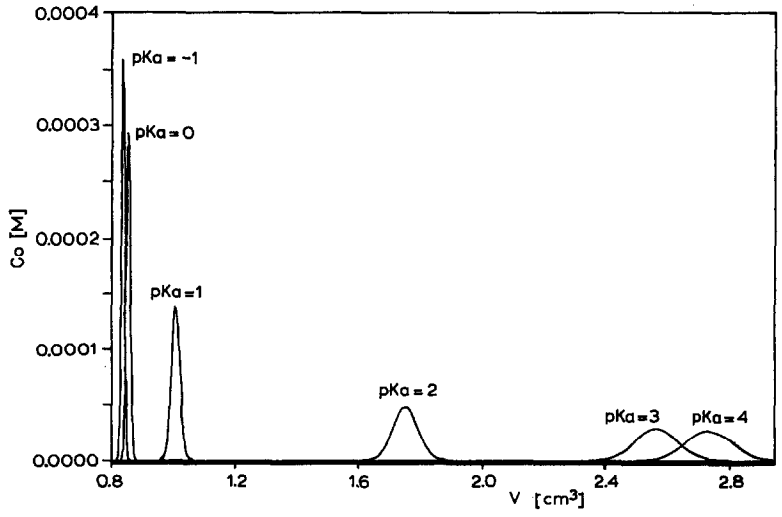

Fig. 10. Chromatograms of several acidic compounds (buffered mobile phase). $c_i = 10^{-3}$ M. Other conditions as in Fig. 7.

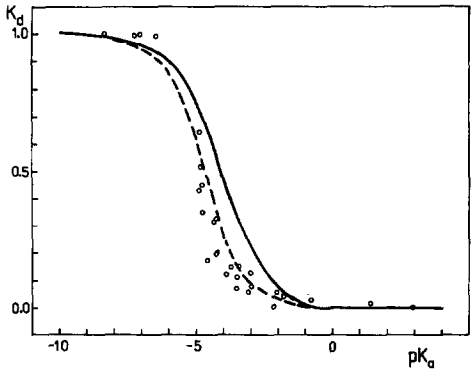

Fig. 11. Dependence of K_d on the logarithm of the acid dissociation constant, pK_a. Solid line: global approach; dashed line: computer modelling; points: experimental values (see Table I, ref. 10). $c_i = 10^{-3}$ *M*. Other conditions as in Fig. 1.

were separated. In the presence of a sufficiently strong and concentrated buffer, all peaks become fairly symmetrical, as has been observed experimentally. The concentration profiles of the sample in the two phases can also be calculated at the time steps of the sample passage down the column. The sample concentration in the stationary phase is never higher than it is in the mobile phase.

We expect the computer simulation to be more accurate and physically correct than the global approach. Therefore it is pleasing that the results obtained in this way are closer to the experimental values as is seen in Fig. 11. The good agreement of the model predictions and the experiment provides support to our ion-exclusion model explaining the primary mechanism of separation of acidic compounds. In real systems however other mechanisms play a role as was described in our previous paper (ref. 10, p. 41).

CONCLUSIONS

Despite its inconsistencies, the global approach describes the experimental facts fairly well. Computer simulations which eliminate these inconsistencies describe the facts even better and provide reasonable predictions on how the addition of the buffer influences the peak shape.

REFERENCES

1 R. H. Wheaton and W. C. Bauman, *Ind. Eng. Chem.*, 45 (1953) 238.
2 G. A. Harlow and D. H. Morman, *Anal. Chem.*, 36 (1964) 2438.
3 P. Jandera and J. Churácek, *J. Chromatogr.*, 86 (1973) 351.
4 H. F. Walton, *Anal. Chem.*, 48 (1976) 52R.
5 W. Czerwiński, *Chem. Anal. (Warsaw)*, 12 (1967) 597.
6 E. Rajakylä, *J. Chromatogr.*, 218 (1981) 695.
7 V. T. Turkelson and M. Richards, *Anal. Chem.*, 50 (1978) 1420.
8 J. Lehotay and M. Traiter, *J. Chromatogr.*, 91 (1974) 261.
9 K. Tanaka, T. Ishizuka and H. Sunahara, *J. Chromatogr.*, 174 (1979) 153.
10 B. K. Głód and W. Kemula, *J. Chromatogr.*, 366 (1986) 39.